ANTICANCER RESEARCH *39*: 1943-1952 (2019)
doi:10.21873/anticanres.13304

Characterization of Bone Lesions in Myeloma Before and During Anticancer Therapy Using ^{18}F-FDG-PET/CT and ^{18}F-NaF-PET/CT

THOMAS SELIM NAKUZ[1], FILIPE PORTELA MILLINGER[1], KAREM EL-RABADI[2], MICHAEL WEBER[2], VERENA PICHLER[1], WOLFGANG WADSAK[1,3], MARKUS MITTERHAUSER[1,4], ALEXANDER HAUG[1], MARCUS HACKER[1], GEORGIOS KARANIKAS[1], PETER PIETSCHMANN[5] and HERMINE AGIS[6]

[1]*Department of Biomedical Imaging and Image-guided Therapy, Division of Nuclear Medicine, Medical University of Vienna, Vienna, Austria;*
[2]*Division of Radiology, Medical University of Vienna, Vienna, Austria;*
[3]*Center for Biomarker Research in Medicine, Graz, Austria;*
[4]*Ludwig Boltzmann Institute of Applied Diagnostics, Vienna, Austria;*
[5]*Department of Pathophysiology and Allergy Research, Center for Pathophysiology, Infectiology and Immunology, Medical University of Vienna, Vienna, Austria;*
[6]*Department of Internal Medicine I, Division of Oncology, Medical University of Vienna, Vienna, Austria*

Abstract. *Background: The objective of this study was to characterize tumor activity and mineralization status in newly-detected multiple myeloma (MM) bone lesions using 2-^{18}F-fluoro-2-deoxy-D-glucose (^{18}F-FDG)-PET/CT and ^{18}F-sodium fluoride (^{18}F-NaF)-PET/CT before and after antitumor treatment. Materials and Methods: In this retrospective study, seven patients with histologically-verified MM were included (four women, three men; median age=57 years, standard deviation=11.23 years). PET/CT was performed with ^{18}F-FDG and with ^{18}F-NaF, both at baseline and after treatment. All patients had positive scans. Volumes of interest (VOIs) were drawn over all ^{18}F-FDG-PET/CT-positive bone lesions, as well as the corresponding regions in ^{18}F-NaF-PET/CT. For characterization of bone lesions, semi-quantitative standard uptake value (SUV) parameters were measured. Results: ^{18}F-FDG-PET/CT in the seven patients detected 39 metabolically active lesions that were correlated with the corresponding sites in ^{18}F-fluoride-PET/CT. Overall, the lesions showed a response to therapy, with a significant decrease in SUV_{max} on PET/CT using ^{18}F-FDG ($p<0.001$) and with ^{18}F-NaF ($p<0.001$). In four patients with a second follow-up scan (at a median of 17 months after baseline scan), there was no significant change in lesion uptake. Conclusion: Based on our data, antitumor therapy in MM reduces not only tumor activity, but also the mineralization status of bone lesions. A second follow-up scan in a subset of the cohort yielded no change in mineralization status.*

Correspondence to: Assoc. Prof. Dr. Georgios Karanikas, Divisional Head PET-PET/CT (Nuclear Medicine), Department of Biomedical Imaging and Image-guided Therapy, Division of Nuclear Medicine, Medical University of Vienna, Waehringer Guertel 18-20, Vienna A-1090, Austria. Tel: +43 14040055500, e-mail: georgios.karanikas@meduniwien.ac.at

Key Words: PET, multiple myeloma, ^{18}F-FDG, ^{18}F-sodium fluoride, positron-emission tomography, PET/CT.

Multiple myeloma (MM) is a neoplastic plasma cell disorder that is characterized by clonal proliferation of malignant plasma cells in the bone marrow (1). Eighty percent of patients experience bone lesions during the course of their disease (1, 2), with focal osteolytic bone lesions being the radiographic hallmark of the disease (3). Changes in the bone microenvironment leads to increased recruitment and activation of osteoclasts and inhibition of osteoblasts (4, 5).

2-^{18}F-Fluoro-2-deoxy-D-glucose (^{18}F-FDG)-PET/CT is a sensitive functional imaging modality for many neoplasm types. The updated International Myeloma Working Group (IMWG) criteria consider focal skeletal lesions with increased ^{18}F-FDG uptake and with osteolytic destruction in the CT component indicative of active myeloma (6). ^{18}F-FDG-PET/CT appears to be especially useful in the evaluation of the quality of treatment response in patients with MM (7-11).

^{18}F-Sodium fluoride (^{18}F-NaF) is a PET tracer used for skeletal imaging which reflects regional blood flow and bone remodeling and can accumulate in osteoblastic and osteolytic

lesions (12-14). Although ^{18}F-NaF is a well-known tracer, its use in PET/CT is considered an intriguing imaging method for the assessment of malignant bone diseases (15-18). Early studies have shown the possibility of using ^{18}F-NaF PET/CT as a valuable tool for diagnosis in MM (19-21). However, several studies have shown this method to have limited performance in the evaluation of myeloma bone disease (22-25). Data about the therapy response, as assessed by ^{18}F-NaF PET/CT is, however, still very limited.

It is well known that the behavior of MM bone lesions changes under therapy (26). The hypothesis of the present study was that in response to therapy, MM bone lesions show increased bone turnover (mineralization) and reduced tumor activity; these changes can be detected with ^{18}F-NaF-PET/CT and ^{18}F-FDG-PET/CT. We expected to detect significant differences in the mineralization of MM bone lesions using ^{18}F-NaF-PET/CT and in tumor activity using ^{18}F-FDG-PET/CT for MM bone lesions before and during therapy.

The aim of this study was to characterize newly-detected MM bone lesions with regard to mineralization status and tumor activity using ^{18}F-/^{18}F-NaF-FDG-PET/CT and conduct a re-evaluation during therapy with these same diagnostic modalities to detect potential changes in the mineralization and tumor activity in MM bone lesions.

Materials and Methods

Patients. Seven patients (four women, three men; median (±standard deviation) age=57±11.23 years; age range=43-78 years) with newly-diagnosed MM, according to the International Myeloma Working Group (IMWG) criteria (6), were retrospectively recruited into the present study. All patients underwent baseline imaging (before anticancer therapy), including standard ^{18}F-FDG-PET/CT with a diagnostic CT component as well as additional ^{18}F-NaF-PET/CT with a low-dose CT component. PET/CT studies were performed within 1 week of each other (five patients underwent both studies on two consecutive days, the remaining 2 within 7 days).

Follow-up imaging, including ^{18}F-NaF-PET/CT and ^{18}F-FDG-PET/CT, was performed after the introduction of anticancer therapy. At least one follow-up study was available for all patients within a median time-frame of 10 months (range=7-13 months). Additional follow-up scans were available for four patients within a median time-frame of 17 months after the baseline scan (range=12-22 months).

This study was approved by the local Ethics Committee (EK-Nr: 1845/2017). Informed consent was obtained from all individual participants included in the study.

Imaging techniques. Both PET tracers, ^{18}F-NaF and ^{18}F-FDG, were prepared on site using standardized protocols on a GE FASTlab synthesizer (GE Healthcare, Boston, MA, USA) with dedicated disposable cassettes on the day of PET/CT imaging. Full radiopharmaceutical quality control according to the monographs of the European Pharmacopoeia was performed prior to product release and patient application.

^{18}F-NaF-PET/CT. PET/CT was performed using a modern hybrid scanner, a Siemens Biograph 64 True Point (Siemens Healthcare Sector, Erlangen, Germany). Helical CT slices and PET emission data were acquired from the skull to the foot in all patients. Image acquisition of emission data was started 30-60 min after *i.v.* injection of 185-370 MBq ^{18}F-NaF. A low-dose CT scan was performed using the following acquisition parameters: 120 kV, 30-40 mAs; slice thickness 1.2 mm; increment 0.7 mm. To match CT slices and PET slices, CT was acquired with the patient in a shallow breathing position. Directly after CT imaging, the PET acquisition protocol was started. Acquisition time was 3 min per bed position (10-12 bed positions per patient). During imaging of the thorax, patients were instructed to maintain shallow breathing. PET images were reconstructed using a CT attenuation correction technique. The reconstruction was performed using the manufacturer's arithmetic reconstruction algorithms ("Iterative 2D uncor. recon" and/or "TrueD cor. recon") in their respective default settings. CT images were converted into linear attenuation coefficients for the 511-keV energy radiation, as implemented in the system. CT and PET images were matched and fused into transaxial and coronal images of 5-mm thickness.

^{18}F-FDG-PET/CT. Using the same hybrid scanner system, data were also acquired from the skull to the foot in all patients. All patients were in a fasting condition for at least 8 h prior to ^{18}F-FDG injection. Serum glucose levels had to range from 80 to 160 mg/dl. Acquisition of emission data was started 60 min after *i.v.* injection of 300-400 MBq of ^{18}F-FDG. A diagnostic CT without contrast medium was performed with the following parameters: 120 kV, 200-230 mAs; slice thickness 3 mm; increment 2 mm. The PET protocol was similar to that of ^{18}F-NaF-PET/CT, with an acquisition time of 3-4 min per bed position (8-12 bed positions per patient). PET and CT images were also reconstructed as described above. CT and PET images were matched and fused into transaxial and coronal images of 5 mm thickness.

Image analysis. Two experienced nuclear medicine physicians analyzed ^{18}F-FDG- and ^{18}F-NaF-PET/CT based on a visual (qualitative) analysis and a semi-quantitative evaluation based on standard uptake value (SUV) calculations.

Qualitative assessment was based on increased focal uptake of ^{18}F-FDG within the bone for which it was possible to exclude benign etiologies (trauma, inflammation, degenerative changes, arthritic disease, *etc*.) and these lesions were considered indicative of MM. ^{18}F-FDG-PET findings were correlated with the CT component, and, in particular, clearly delineated osteolytic lesions were considered proof of myelomatous lesions according to IMWG guidelines (6). In addition, increased homogenous, diffuse bone marrow uptake of ^{18}F-FDG on maximum intensity projections was considered indicative of myeloma. To minimize false-positive assessment, patient history was studied thoroughly. ^{18}F-FDG-PET/CT-positive lesions were correlated with those of ^{18}F-NaF-PET/CT and served as a reference standard for this study, as there is no systemized standard for the evaluation of myelomatous lesions with this modality.

Semi-quantitative assessment was based on volumes of interest (VOIs) drawn semi-automatically using threshold-based delineation provided by the image analysis software (Hybrid 3D™ Viewer; Hermes Medical Solutions, Stockholm, Sweden), which was adjusted manually for optimal correlation with osteolytic bone

Table I. *Demographic data, initial histology, treatment cycles, and responses of study patients.*

		Initial histology*			Treatment cycle 1			Treatment cycle 2		
Case no.	Age, years†	R-ISS stage	Grade	PCI	Treatment	Serological response	Imaging response	Treatment	Serological response	Imaging response
1	43	2	2	80%	RTX, I-CTX, ASCT	CR	PD	I-CTX	PD‡	PD
2	64	1	1	60%	RTX, I-CTX	CR	SD	ASCT	CR	SD
3	50	1	2	90%	I-CTX, ASCT	CR	PR	Bortezomib	CR	SD
4	78	1	2	50%	RTX, I-CTX	CR	CR	-	-	-
5	53	1	2	20%	I-CTX	VGPR	PR	No therapy	CR	SD
6	57	3	2	50%	I-CTX, ASCT	CR	PR	-	-	-
7	70	1§	2	90%	RTX, I-CTX	VGPR	SD	-	-	-

R-ISS stage: Revised International Staging System for Multiple Myeloma (29); PCI: plasma cell infiltration; RTX: radiotherapy; I-CTX: immunochemotherapy; ASCT: autologous stem cell transplantation; CR: complete response; VGPR: very good partial response; PR: partial response; SD: stable disease. *All histological samples were taken from the iliac bone; †At baseline scan. ‡This patient had an initial CR to treatment, but eventually showed relapse. §R-ISS stage only determined after the beginning of treatment.

destruction at the initial scan. Due to the very good response shown by the majority of patients after treatment, no focal ^{18}F-FDG-uptake was detectable in some of the patients at follow-up. In these cases, cubic VOIs with a volume of 3 ml were placed either within osteolytic lesions detectable on CT or according to the anatomy of the initially metabolically active lesion.

Reference regions for the blood pool in the upper mediastinum and for bone metabolism using the fourth lumbar vertebra (L4), or iliac bone, if the previous region was affected, were drawn as cubic volumes of 10 ml and 3 ml, respectively. These VOIs served as reference tissue values for ^{18}F-FDG-PET and ^{18}F-NaF-PET lesions, respectively, to calculate the tumor-to-background ratio (TBR).

Patient-based therapy assessment was conducted according to the European Organization for Research and Treatment of Cancer (EORTC) 1999 criteria, which define four treatment response groups: Complete response (CR, with complete resolution of ^{18}F-FDG uptake indistinguishable from the surroundings); partial response (PR); stable disease (SD); and progressive disease (PD) (27).

Clinical and histological data acquisition. Data about therapy, plasma cell infiltration status, and laboratory parameters were collected at the initial PET/CT scan and at each follow-up. Clinical therapy response was assessed according to the modified IMWG response criteria for MM (28).

Statistical analysis. Data were statistically evaluated using SPSS 24.0 (IBM, Armonk, NY, USA) software. The statistical evaluation was performed using descriptive statistics and a mixed model analysis of variance (ANOVA), as well as Pearson's correlation. Results were considered significant for p-values less than 0.05 ($p<0.05$).

Results

Seven patients (four women, three men; median age=57±11.23 years) newly diagnosed with MM were retrospectively recruited between March 2013 and October 2014 at the General Hospital of Vienna. All patients were followed-up for at least 30 months (median=45 months, range=21-53 months), with the exception of one patient who died 9 months after the first follow-up scan (Table I).

The initial stage, according to the Revised International Staging System for Multiple Myeloma (R-ISS) (29), was stage 1 for five patients and stage 2 and stage 3 for one patient. For one patient with R-ISS stage I, serological data to determine the stage was found only after the induction of anticancer therapy. Initial bone marrow biopsy in the iliac bone was positive for all patients, with one patient demonstrating a grade 1 plasma cell myeloma and the remaining six patients demonstrating a grade 2 plasma cell myeloma. The bone marrow showed a median infiltration of 60±23.7% (range=20-90%). Four patients were classified as having light-chain myelomas (two κ- and two λ-light-chain myelomas each) and the remaining as IgG myelomas (two κ- and one λ-IgG myelomas) (Table I).

After the initial PET/CT assessments, all patients underwent immunochemotherapy with a bortezomib-containing regimen. Four patients received additional local radiotherapy (57.1%) and three patients received autologous stem cell transplantation (ASCT) (42.9%).

After anticancer therapy, all patients showed either a very good PR or CR according to the IMWG guidelines (28), two and five patients, respectively. Bone marrow infiltration after therapy was reported to be either <5% or at 5%, with histological data missing for one patient (Table I).

The four patients who underwent a second follow-up scan all received different therapies after the first follow-up scan. One patient initially underwent ASCT. One patient received consolidating immunotherapy, while another received a second dose of immunochemotherapy. The last patient received no treatment. Three patients showed CR to the therapy. The fourth patient who underwent a second treatment-cycle of immunochemotherapy initially showed

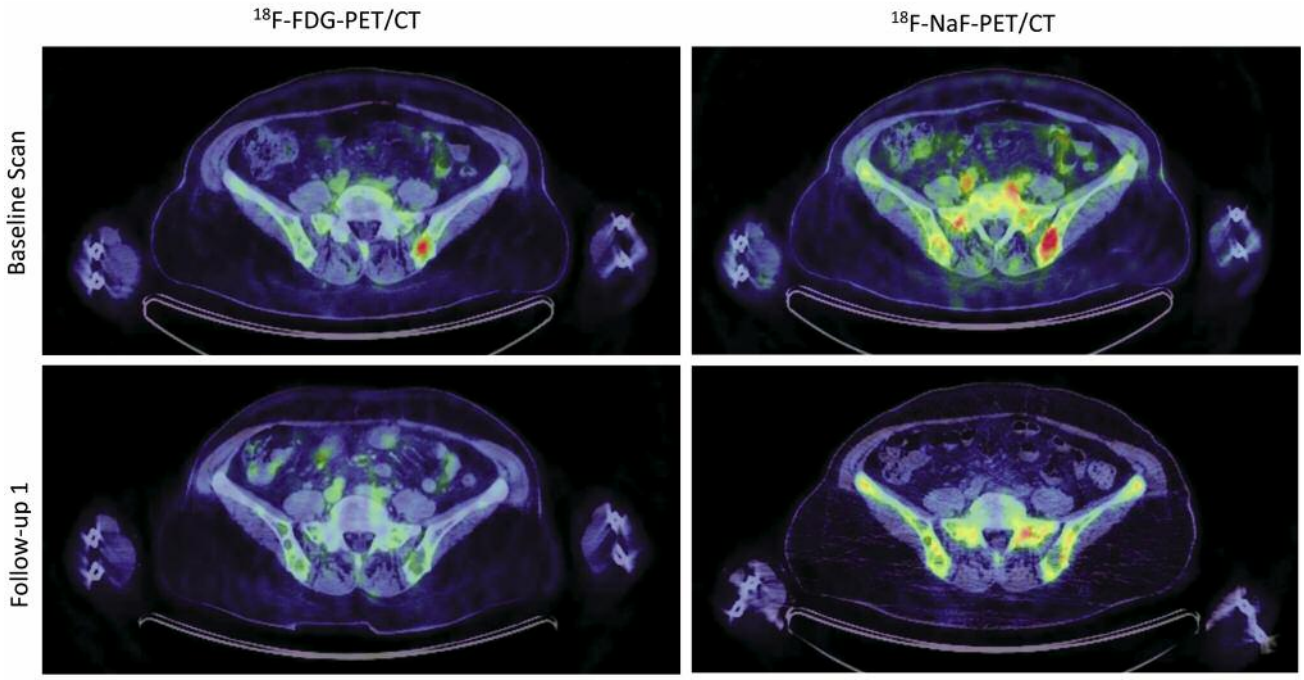

Figure 1. *2-^{18}F-Fluoro-2-deoxy-D-glucose (^{18}F-FDG)-PET/CT and ^{18}F-sodium fluoride (^{18}F-NaF)-PET/CT for patient 6 with a metabolically active lesion in the left os ilium at the baseline scan. The lesion shows marked ^{18}F-FDG (upper left) and ^{18}F-NaF uptake (upper right). After anticancer therapy (immunochemotherapy and autologous stem cell transplantation), there was a significant decrease in tracer uptake on both ^{18}F-FDG-PET/CT (lower left) and ^{18}F-NaF-PET/CT (lower right).*

CR but presented with serological relapse before the second follow-up scan (Table I).

Baseline ^{18}F-FDG-PET/CT revealed 34 lesions in six patients. One patient showed diffuse bone marrow uptake, with no clearly defined focal lesions. Five areas of interest were then determined based on Positron-Emission Tomography Response Criteria in Solid Tumors (PERCIST) criteria (30), which determines a set number of five lesions for therapy response assessment based on peak standard uptake values using lean body mass (SUL_{peak}).

^{18}F-NaF-PET/CT showed correlating focal uptake in 28 lesions in six patients. Other patterns of uptake were diffuse pattern, correlating the ^{18}F-FDG-PET/CT in the patient with diffuse bone marrow uptake. Two lesions were ^{18}F-NaF-negative, one within the marrow of the proximal femur of one patient, the other in the sacrum of another patient. Finally, elevated ^{18}F-NaF in the bone adjacent to the FDG-avid focus was seen in four lesions of one patient.

The four patients with second follow-up PET/CTs initially had a total of 21 ^{18}F-FDG-positive lesions, including one patient with only one lesion and the aforementioned patient with diffuse bone marrow uptake.

After the initial treatment cycle, therapy response assessment by ^{18}F-FDG-PET/CT according to EORTC guidelines (27) showed CR in one patient, PR in three patients, SD in two patients and PD in one patient (Figure 1). The patient with PD showed serological CR and displayed reduced ^{18}F-FDG uptake but a new paravertebral lesion was discovered on the follow-up scan. Of the four patients with a second follow-up scan, three patients showed SD compared to the first follow-up having initially shown either PR or SD. The patient with PD initially showed an increase in ^{18}F-FDG uptake in the known lesions compared to that at the first follow-up and additionally displayed newly diagnosed extramedullary disease in the vesical urinaria, thus showing PD once more. However, the SUV values for this patient did not reach the levels of the initial baseline scan.

In ^{18}F-NaF-PET/CT treatment responses based on EORTC guidelines (27) showed partial response in all but one patient. Patient 7 showed PD with an actual increase in mineralization after treatment with radiotherapy and immuneochemotherapy. In the four patients with a second follow-up, the scans all showed SD compared to the first follow-up.

In addition to SUV values based on body weight, SUV based on body surface area [as recommended in the EORTC guidelines (27), as well as SUV based on lean body mass [SUL, as recommended in the PERCIST

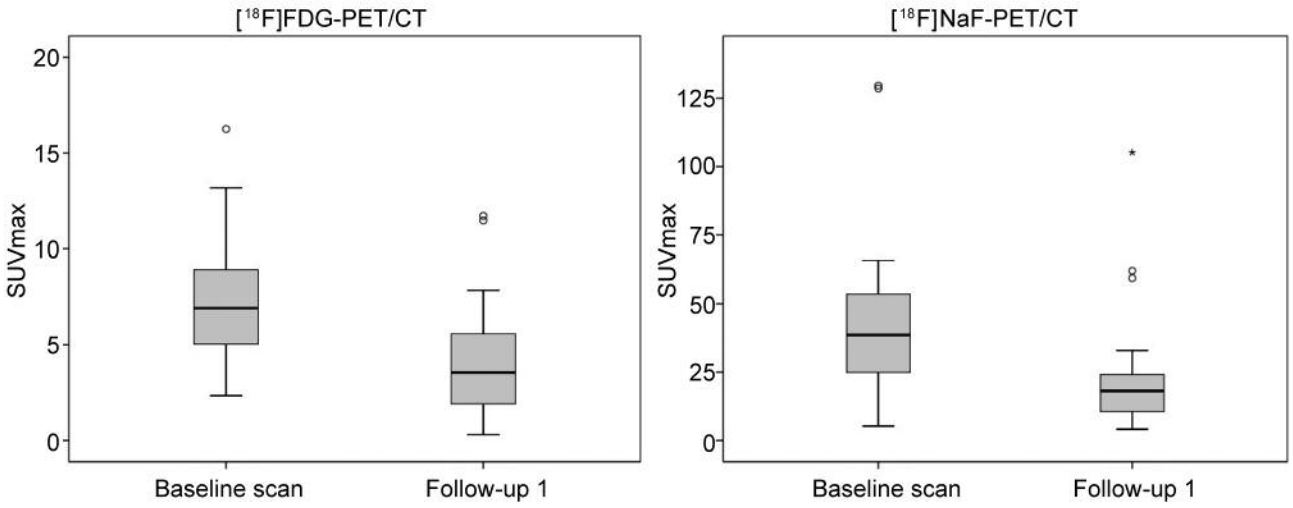

Figure 2. *Maximum standard uptake value (SUV_{max}) before (A) and after (B) anticancer therapy. Changes were significant ($p<0.001$) on both ^{18}F-FDG-PET/CT and ^{18}F-NaF-PET/CT.*

guidelines (30)], were measured. For ^{18}F-FDG-PET/CT, SUV_{max} and SUV_{peak} were measured, as a reproducible SUV_{mean} would not have been achievable in patients with CR after initial therapy. For ^{18}F-NaF-PET/CT, SUV_{max}, SUV_{peak}, and SUV_{mean} were measured, as many lesions still showed focal uptake after the initial anticancer therapy. Correlation of SUV_{max} with SUV_{peak} and SUV_{mean} (in the case of ^{18}F-NaF-PET/CT) yielded a high correlation of >0.9 in almost all cases except one. Similarly, SUV values based on body weight, body surface area, and lean body mass also showed a high correlation. For this reason, we decided to use only SUV_{max} based on body weight in our descriptive analysis, as it is the most commonly used parameter in the literature.

A mixed model ANOVA showed a significant decrease of SUV_{max} in the myeloma lesions before and after therapy on ^{18}F-FDG-PET/CT ($p<0.001$). The average SUV_{max} at the initial scan was 7.19±3.15. After therapy, the mean SUV_{max} decreased to 3.96±2.78. ^{18}F-NaF-PET/CT also showed a significant decrease in SUV_{max} ($p<0.001$). Mean SUV_{max} decreased from 41.71±26.58 to 21.95±18.44. Pearson's correlation showed a significant but weak positive correlation between relative changes in SUV_{max} between ^{18}F-FDG-PET/CT and ^{18}F-NaF-PET/CT, with a correlation coefficient of 0.363 (p=0.023). No significant changes in SUV_{max} were found between the first and second follow-up on either ^{18}F-FDG- or ^{18}F-NaF-PET/CT ($p>0.99$) (Figure 2).

When correcting for background activity using the upper mediastinum as the blood pool reference for ^{18}F-FDG and, when available, L4 or the left iliac bone for ^{18}F-NaF as normal bone uptake, there remained a significant decrease between baseline and the first follow-up ($p<0.001$ for both modalities). One patient with a diffuse pattern of uptake in the bone marrow had to be excluded from TBR calculations for ^{18}F-NaF because it was not possible to establish healthy bone reference tissue in either the lumbar spine nor the hip. The TBR at the first and second follow-up continued to show no significant difference ($p>0.99$). The average TBR at baseline was significantly different from those at the first and second follow-ups but did not differ significantly between the follow-up studies in either ^{18}F-FDG-PET/CT and ^{18}F-NaF-PET/CT as seen in Table II.

In ^{18}F-FDG-PET/CT, the standard deviation at baseline for intra-patient SUV_{max} was lower than that for the combined lesion pool (1.20-1.96 compared to 3.15), suggesting a more homogenous lesion activity for each patient. ^{18}F-NaF-PET/CT displayed a wider range of standard deviations from 3.91-37.23. Treatment response in both modalities tended toward a lower standard deviation but notable exceptions were present in both. While treatment response was displayed in all but one patient and ^{18}F-FDG and ^{18}F-NaF uptake decreased significantly, not all lesions displayed similar responses when looked at individually. In the first follow-up, all but one initially ^{18}F-FDG-avid lesion showed reduced uptake to varying degrees. In ^{18}F-NaF, six lesions displayed increased uptake including the lesion that had increased ^{18}F-FDG uptake. Two lesions in patient 7 showed a marked increase in SUV_{max}, leading to this patient being evaluated as having PD. The four patients with a second follow-up study displayed a much more varied response for each individual lesion in that follow-up.

Table II. *Average (± SD) maximum standard uptake value (SUV_{max}) and tumor–to–background ratio (TBR) values for all lesions.*

Timepoint	^{18}F-FDG				^{18}F-NaF			
	SUV_{max}	*p*-Value*	TBR†	*p*-Value*	SUV_{max})	*p*-Value*	TBR‡	*p*-Value*
Baseline	7.19 (±3.15)		1.77 (±0.28)		41.71 (±26.58)		11.11 (±3.12)	
Follow-up 1 (n=39)	3.96 (±2.78)	<0.001	1.07 (±0.44)	0.001	21.95 (±18.44)	<0.001	3.24 (±1.96)	<0.001
Follow-up 2 (n=21)	4.20 (±1.35)	<0.001	1.02 (±0.57)	0.006	23.55 (±17.92)	<0.001	4.58 (±2.93)	0.002

FDG: Fluoro-2-deoxy-D-glucose; SD: standard deviation. **Versus* baseline PET/CT. Reference tissue: †mediastinum (10 ml volume-of-interest), ‡fourth lumbar vertebrae (3 ml volume-of-interest); one patient had to be excluded due to manifestations of diffuse myeloma.

Discussion

MM is the second most prevalent hematological malignancy after non-Hodgkin's lymphoma (31) and many studies have shown ^{18}F-FDG-PET/CT to be useful, especially in evaluation of treatment response, which led to its inclusion in IMWG guidelines (6). ^{18}F-NaF-PET/CT, however, has only recently been studied as a potential diagnostic tool for the detection of myelomatous lesions, mostly with disappointing results (22-25, 32). There are only limited data about the changes in ^{18}F-NaF uptake before and after therapy.

In our study, there was a significant reduction in ^{18}F-NaF uptake after first-line therapy. Subsequent follow-up scans did not show any significant changes in either ^{18}F-FDG-PET/CT or ^{18}F-NaF-uptake. However, TBRs (using bone and the blood pool for ^{18}F-NaF-PET/CT and ^{18}F-FDG-PET/CT, respectively) continued to show an increased tracer uptake in ^{18}F-NaF-PET/CT, indicating reduced but active mineralization processes after treatment. It is well known that the bone microenvironment is altered in the course of MM, leading to an environment that is osteoblast-inhibiting, osteoclastogenic, and in which osteoclast activity is promoted (4, 5, 33). However, the mechanisms that underlie the persistence of osteolytic lesions, even in responding patients, and the continued suppression of osteoclasts, are not well understood. In our study, we showed an effect of therapy on bone mineralization, but no significant changes between subsequent follow-ups even in patient 5 (one lesion) who received no further therapy after the initial regimen (SUV_{max} 9.54 and 10.52 at the first and second follow-ups, respectively).

Two studies have looked into ^{18}F-NaF-PET/CT in MM before and after therapy. In 2017, Wang *et al*. released initial data describing ^{18}F-NaF uptake as a surrogate marker for bone metabolism in patients undergoing treatment with Dickkopf-related protein 1 (DKK1)-inhibiting monoclonal antibodies. A small number of patients underwent static and dynamic ^{18}F-NaF-PET/CT as well as dual-energy X-ray absorptiometry before and after six cycles of DKK1-inhibiting monoclonal antibody therapy. The mean SUV in the lumbar spine and left hip was measured in static PET/CT and tracer accumulation in the 10th thoracic vertebra in dynamic PET/CT. The results showed a stable or increasing uptake of ^{18}F-NaF after six cycles of therapy and an increase in bone mineral density after therapy. No pathological lesions were measured (34). Comparisons with our study show similar average SUV_{mean} values for the fourth lumbar vertebra at baseline scan but with a higher range [4.60 (range=0.59-8.53 compared to 5.0 (range=4.0-6.9)]. After anticancer therapy, SUV_{mean} values dropped in our cohort while a rise was noted in the cohort treated with the DKK1-inhibiting monoclonal antibody [3.81 (range=1.59-7.27) compared to 5.6 (range=4.4-7.2)]. Another point of difference is the fact that our patient cohort was treated with first line therapy while disease in all the patients receiving the antibody was refractory or relapsed with at least one line of therapy (34). Interestingly, the four patients with a second follow-up scan and vastly different treatment regimens showed average SUV_{mean} values and ranges similar to those of the baseline scan [4.68 (range=0.55-8.17)].

In 2017, Sachpekidis *et al*. evaluated 29 patients using static and dynamic ^{18}F-FDG-PET/CT and ^{18}F-NaF-PET/CT before and after high-dose chemotherapy and ASCT. ^{18}F-FDG-positive lesions were used as a gold standard and were correlated to ^{18}F-NaF-positive lesions in the same way as in our study. Therapy assessment was made using EORTC guidelines (27) for both ^{18}F-FDG-PET/CT and ^{18}F-NaF-PET/CT. ^{18}F-NaF-PET/CT revealed significantly fewer myelomatous lesions when compared to ^{18}F-FDG-PET/CT, a result that was not reproducible in our study. Overall changes in therapy response were less pronounced than in our study, with the majority of patients showing SD and a number of patients showing PD that correlated with either PR or PD on ^{18}F-FDG-PET/CT. In our study, using the same guidelines for ^{18}F-NaF-PET/CT as for ^{18}F-FDG-PET/CT, all of our patients except one showed PR. Patient 7 showed a marked increase in ^{18}F-NaF uptake in two lesions while exhibiting reduced uptake in the other two lesions, as well as in the reference tissue. Patient 7 showed SD in the corresponding ^{18}F-FDG-PET/CT. Semi-quantitative (SUV_{max}) and kinetic parameters showed a significant decrease after therapy, similarly to our study, but to a lesser extent (25). A

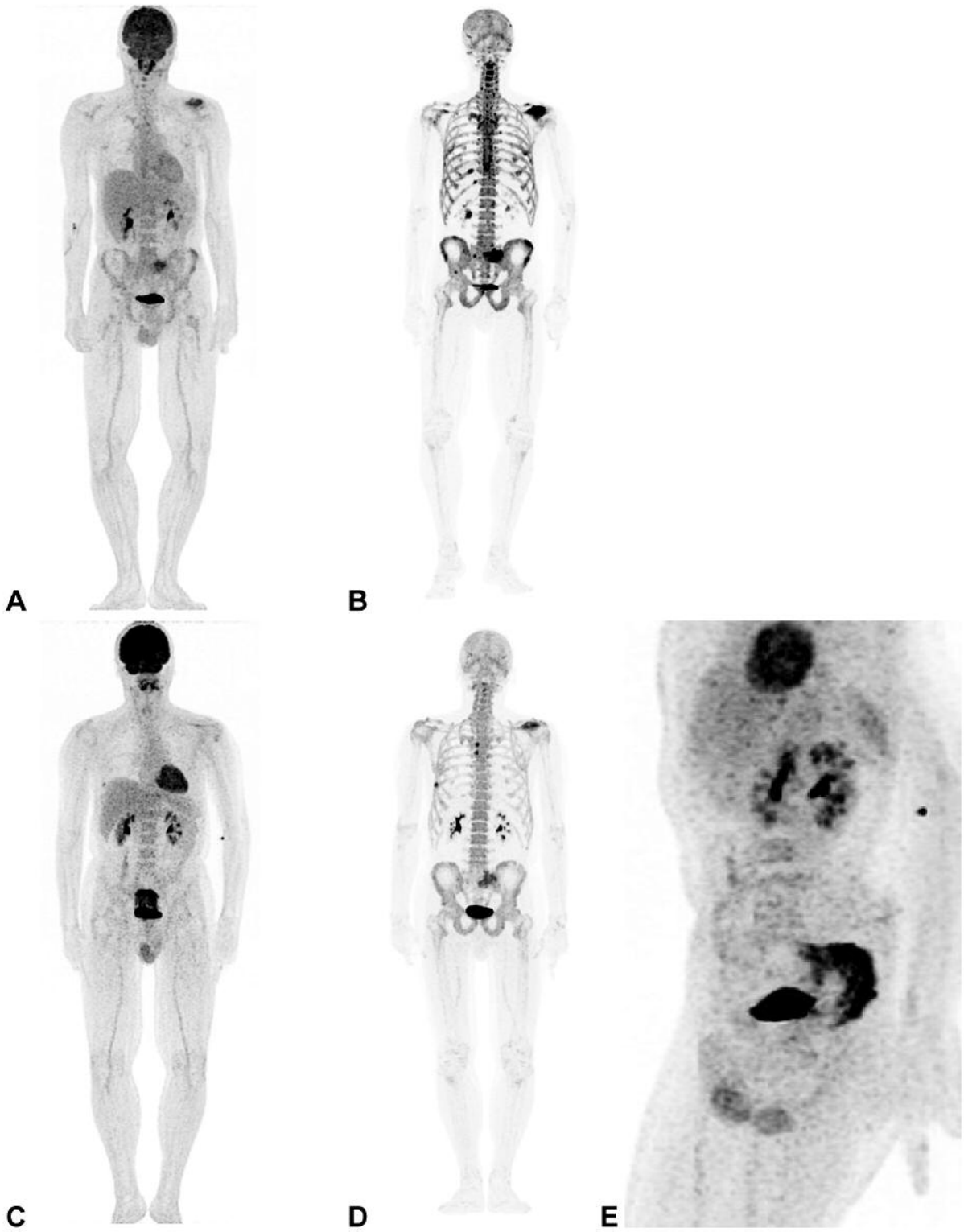

Figure 3. *Maximum intensity projection (MIP) images of patient 1. A: Baseline 2-18F-fluoro-2-deoxy-D-glucose (^{18}F-FDG)-PET/CT; the lesions in the left clavicle and the left massa lateralis can be clearly seen. B: Baseline ^{18}F-sodium fluoride (^{18}F-NaF)-PET/CT correlation of lesions. C: Follow-up 18F-FDG-PET/CT showed a marked decrease in the known bone metastases and revealed a new paravertebral lesion. D: Follow-up 18F-NaF-PET/CT showing marked decrease in the known lesions. The newly found lesion in ^{18}F-FDG-PET/CT did not show any uptake. E: Oblique view of the ^{18}F-FDG-PET/CT follow-up scan allowed a better appreciation of the newly found lesion.*

marked difference in the two study cohorts is the larger number of patients in the study of Sachpekidis *et al*. and the uniform therapy regimen. All patients received high-dose chemotherapy with melphalan and ASCT before the second scan. In our study, only three patients received ASCT before the first scan while all received immunochemotherapy, including bortezomib, as the first-line treatment. Treatment response in ^{18}F-FDG-PET/CT was 48.3% CR, 37.9% PR, and 13.8% PD in the study of Sachpekidis *et al*. and correspondingly 14.3%, 42.9%, 28.6%, and 14.3% in our study.

With regard to treatment response using ^{18}F-FDG-PET/CT, patient 1 showed interesting results. This patient, with an initial ISS stage of 2 and IgG-myeloma, showed a serological CR after initial anticancer therapy. However, he showed progression on the follow-up scan, with a new ^{18}F-FDG-avid paravertebral lesion (Figure 3). Two months after the follow-up scans, IgG paraproteins started to rise again and the decision to perform a second line of immunochemotherapy was made. Literature studies have shown the value of ^{18}F-FDG-PET/CT in treatment response evaluation with regard to overall survival and progression-free survival (35, 36), leading to its inclusion in the IMWG guidelines (6).

This study has certain limitations. The small number of patients in this cohort, the inhomogeneous treatment regimens, and the varying times of follow-up scans limit the possibilities of statistical analysis of certain therapy effects. As discussed above, longer follow-up with later scans might have revealed different uptake dynamics in ^{18}F-NaF-PET/CT. The lack of standardized criteria with which to evaluate ^{18}F-NaF uptake is a further limitation.

Conclusion

Baseline and post-therapy ^{18}F-FDG-PET/CT and ^{18}F-NaF-PET/CT in this study demonstrated the excellent therapy response-evaluation properties of ^{18}F-FDG-PET/CT that have been shown repeatedly in the literature. ^{18}F-NaF-PET/CT as a marker of bone mineralization was shown to be significantly decreased after first-line therapy in our study population, but no significant changes were detected between the first and second follow-up scans. Larger studies are needed to study ^{18}F-NaF-PET/CT uptake dynamics over a longer period of time to show whether permanent changes in the bone microenvironment can be reliably shown with this tracer, which may lead to changes in treatment approaches for this disease.

Compliance with Ethical Standards

This study received no funding.

Conflicts of Interest

The Authors declare no conflict of interest in regard to this study.

Authors' Contributions

TN analyzed and interpreted the data and wrote the article. FP collected the data and aided in the image analysis. KE review the imaging data. MW executed the statistical analysis. VP, WW and MM provided the tracer and reviewed and corrected the parts of this article regarding chemical nomenclature and tracer production. AH and MH reviewed and corrected the article for intellectual content. GK serves as the Corresponding Author and primary investigator of this study. PP and HM reviewed and corrected this article for intellectual content in regards to accuracy of statements regarding haematology and pathology.

References

1 Palumbo A and Anderson K: Multiple myeloma. N Engl J Med *364(11)*: 1046-1060, 2011. PMID: 21410373. DOI: 10.1056/NEJMra1011442

2 Kyle RA, Gertz MA, Witzig TE, Lust JA, Lacy MQ, Dispenzieri A, Fonseca R, Rajkumar SV, Offord JR, Larson DR, Plevak ME, Therneau TM and Greipp PR: Review of 1027 patients with newly diagnosed multiple myeloma. Mayo Clin Proc *78(1)*: 21-33, 2003. PMID: 12528874. DOI: 10.4065/78.1.21

3 Walker RC, Brown TL, Jones-Jackson LB, De Blanche L and Bartel T: Imaging of multiple myeloma and related plasma cell dyscrasias. J Nucl Med *53(7)*: 1091-1101, 2012. PMID: 22693310. DOI: 10.2967/jnumed.111.098830

4 Terpos E and Dimopoulos M-A: Myeloma bone disease: pathophysiology and management. Ann Oncol *16(8)*: 1223-1231, 2005. PMID: 15928069. DOI: 10.1093/annonc/mdi235

5 Roodman GD: Pathogenesis of myeloma bone disease. J Cell Biochem *109(2)*: 283-291, 2009. PMID: 20014067. DOI: 10.1002/jcb.22403

6 Rajkumar SV, Dimopoulos MA, Palumbo A, Blade J, Merlini G, Mateos M-V, Kumar S, Hillengass J, Kastritis E, Richardson P, Landgren O, Paiva B, Dispenzieri A, Weiss B, LeLeu X, Zweegman S, Lonial S, Rosinol L, Zamagni E, Jagannath S, Sezer O, Kristinsson SY, Caers J, Usmani SZ, Lahuerta JJ, Johnsen HE, Beksac M, Cavo M, Goldschmidt H, Terpos E, Kyle RA, Anderson KC, Durie BG and Miguel JF: International Myeloma Working Group updated criteria for the diagnosis of multiple myeloma. Lancet Oncol *15(12)*: e538-548, 2014. PMID: 25439696. DOI: 10.1016/S1470-2045(14)70442-5

7 Cavo M, Terpos E, Nanni C, Moreau P, Lentzsch S, Zweegman S, Hillengass J, Engelhardt M, Usmani SZ, Vesole DH, San-Miguel J, Kumar SK, Richardson PG, Mikhael JR, da Costa FL, Dimopoulos MA, Zingaretti C, Abildgaard N, Goldschmidt H, Orlowski RZ, Chng WJ, Einsele H, Lonial S, Barlogie B, Anderson KC, Rajkumar SV, Durie BGM and Zamagni E: Role of ^{18}F-FDG PET/CT in the diagnosis and management of multiple myeloma and other plasma cell disorders: a consensus statement by the International Myeloma Working Group. Lancet Oncol *18(4)*: e206-217, 2017. PMID: 28368259. DOI: 10.1016/S1470-2045(17)30189-4

8 Nanni C and Zamagni E: Therapy assessment in multiple myeloma with PET. Eur J Nucl Med Mol Imaging *44(S1)*: 111-117, 2017. PMID: 28573329. DOI: 10.1007/s00259-017-3730-4

9 Nanni C, Zamagni E, Celli M, Caroli P, Ambrosini V, Tacchetti P, Brioli A, Zannetti B, Pezzi A, Pantani L, Perrone G, Zompatori M, Cavo M, Colletti PM, Rubello D and Fanti S: The value of ^{18}F-FDG PET/CT after Autologous stem cell transplantation (ASCT) in patients affected by multiple myeloma (MM). Clin Nucl Med *38(2)*: e74-79, 2013. PMID: 23143049. DOI: 10.1097/RLU.0b013e318266cee2

10 Zamagni E, Patriarca F, Nanni C, Zannetti B, Englaro E, Pezzi A, Tacchetti P, Buttignol S, Perrone G, Brioli A, Pantani L, Terragna C, Carobolante F, Baccarani M, Fanin R, Fanti S and Cavo M: Prognostic relevance of 18-F FDG PET/CT in newly diagnosed multiple myeloma patients treated with up-front autologous transplantation. Blood *118(23)*: 5989-5995, 2011. PMID: 21900189. DOI: 10.1182/blood-2011-06-361386

11 Caldarella C, Treglia G, Isgrò MA, Treglia I and Giordano A: The role of fluorine-18-fluorodeoxyglucose positron emission tomography in evaluating the response to treatment in patients with multiple myeloma. Int J Mol Imaging *2012*: 1-6, 2012. PMID: 22928100. DOI: 10.1155/2012/175803

12 Blau M, Ganatra R and Bender MA: ^{18}F-fluoride for bone imaging. Semin Nucl Med *2(1)*: 31-37, 1972. PMID: 5059349.

13 Hawkins RA, Choi Y, Huang SC, Hoh CK, Dahlbom M, Schiepers C, Satyamurthy N, Barrio JR and Phelps ME: Evaluation of the skeletal kinetics of fluorine-18-fluoride ion with PET. J Nucl Med *33(5)*: 633-642, 1992. PMID: 1569473.

14 Czernin J, Satyamurthy N and Schiepers C: Molecular mechanisms of bone ^{18}F-NaF deposition. J Nucl Med *51(12)*: 1826-1829, 2010. PMID: 21078790. DOI: 10.2967/jnumed.110.077933

15 Hillner BE, Siegel BA, Hanna L, Duan F, Quinn B and Shields AF: ^{18}F-fluoride PET used for treatment monitoring of systemic cancer therapy: Results from the National Oncologic PET Registry. J Nucl Med *56(2)*: 222-228, 2015. PMID: 25593113. DOI: 10.2967/jnumed.114.150391

16 Even-Sapir E, Mishani E, Flusser G and Metser U: ^{18}F-fluoride positron emission tomography and positron emission tomography/computed tomography. Semin Nucl Med *37(6)*: 462-469, 2007. PMID: 17920353. DOI: 10.1053/j.semnuclmed. 2007.07.002

17 Lecouvet FE, Talbot JN, Messiou C, Bourguet P, Liu Y, de Souza NM and EORTC Imaging Group: Monitoring the response of bone metastases to treatment with Magnetic Resonance Imaging and nuclear medicine techniques: a review and position statement by the European Organisation for Research and Treatment of Cancer imaging group. Eur J Cancer *50(15)*: 2519-2531, 2014. PMID: 25139492. DOI: 10.1016/j.ejca.2014.07.002

18 Grant FD, Fahey FH, Packard AB, Davis RT, Alavi A and Treves ST: Skeletal PET with ^{18}F-fluoride: Applying new technology to an old tracer. J Nucl Med *49(1)*: 68-78, 2008. PMID: 18077529. DOI: 10.2967/jnumed.106.037200

19 Nishiyama Y, Tateishi U, Shizukuishi K, Shishikura A, Yamazaki E, Shibata H, Yoneyama T, Ishigatsubo Y and Inoue T: Role of ^{18}F-fluoride PET/CT in the assessment of multiple myeloma: initial experience. Ann Nucl Med *27(1)*: 78-83, 2013. PMID: 22914967. DOI: 10.1007/s12149-012-0647-7

20 Xu F, Liu F and Pastakia B: Different lesions revealed by ^{18}F-FDG PET/CT and ^{18}F-NaF PET/CT in patients with multiple myeloma. Clin Nucl Med *39(9)*: e407-409, 2014. PMID: 24217536. DOI: 10.1097/RLU.0000000000000285

21 Oral A, Yazici B, Ömür Ö, Comert M and Saydam G: ^{18}F-FDG and ^{18}F-NaF PET/CT findings of a multiple myeloma patient with thyroid cartilage involvement. Clin Nucl Med *40(11)*: 873-876, 2015. PMID: 26204214. DOI: 10.1097/RLU.0000 000000000908

22 Sachpekidis C, Goldschmidt H, Hose D, Pan L, Cheng C, Kopka K, Haberkorn U and Dimitrakopoulou-Strauss A: PET/CT studies of multiple myeloma using ^{18}F-FDG and ^{18}F-NaF: comparison of distribution patterns and tracers' pharmacokinetics. Eur J Nucl Med Mol Imaging *41(7)*: 1343-1353, 2014. PMID: 24562650. DOI: 10.1007/s00259-014-2721-y

23 Ak İ, Onner H and Akay OM: Is there any complimentary role of F-18 NaF PET/CT in detecting of osseous involvement of multiple myeloma? A comparative study for F-18 FDG PET/CT and F-18 FDG NaF PET/CT. Ann Hematol *94(9)*: 1567-1575, 2015. PMID: 26068066. DOI: 10.1007/s00277-015-2410-3

24 Bhutani M, Turkbey B, Tan E, Korde N, Kwok M, Manasanch EE, Tageja N, Mailankody S, Roschewski M, Mulquin M, Carpenter A, Lamping E, Minter AR, Weiss BM, Mena E, Lindenberg L, Calvo KR, Maric I, Usmani SZ, Choyke PL, Kurdziel K and Landgren O: Bone marrow abnormalities and early bone lesions in multiple myeloma and its precursor disease: a prospective study using functional and morphologic imaging. Leuk Lymphoma *57(5)*: 1114-1121, 2016. PMID: 26690712. DOI: 10.3109/10428194.2015.1090572

25 Sachpekidis C, Hillengass J, Goldschmidt H, Wagner B, Haberkorn U, Kopka K and Dimitrakopoulou-Strauss A: Treatment response evaluation with ^{18}F-FDG PET/CT and ^{18}F-NaF PET/CT in multiple myeloma patients undergoing high-dose chemotherapy and autologous stem cell transplantation. Eur J Nucl Med Mol Imaging *44(1)*: 50-62, 2017. PMID: 27573638. DOI: 10.1007/s00259-016-3502-6

26 Röllig C, Knop S and Bornhäuser M: Multiple myeloma. Lancet *385(9983)*: 2197-2208, 2015. PMID: 25540889. DOI: 10.1016/S0140-6736(14)60493-1

27 Young H, Baum R, Cremerius U, Herholz K, Hoekstra O, Lammertsma AA, Pruim J and Price P: Measurement of clinical and subclinical tumour response using ^{18}F-fluorodeoxyglucose and positron emission tomography: review and 1999 EORTC recommendations. European Organization for Research and Treatment of Cancer (EORTC) PET Study Group. Eur J Cancer *35(13)*: 1773-1782, 1999. PMID: 10673991

28 Durie BGM, Harousseau J-L, Miguel JS, Bladé J, Barlogie B, Anderson K, Gertz M, Dimopoulos M, Westin J, Sonneveld P, Ludwig H, Gahrton G, Beksac M, Crowley J, Belch A, Boccadaro M, Cavo M, Turesson I, Joshua D, Vesole D, Kyle R, Alexanian R, Tricot G, Attal M, Merlini G, Powles R, Richardson P, Shimizu K, Tosi P, Morgan G, Rajkumar SV and International Myeloma Working Group: International uniform response criteria for multiple myeloma. Leukemia *20(9)*: 1467-1473, 2006. PMID: 16855634. DOI: 10.1038/sj.leu.2404284

29 Palumbo A, Avet-Loiseau H, Oliva S, Lokhorst HM, Goldschmidt H, Rosinol L, Richardson P, Caltagirone S, Lahuerta JJ, Facon T, Bringhen S, Gay F, Attal M, Passera R, Spencer A, Offidani M, Kumar S, Musto P, Lonial S, Petrucci MT, Orlowski RZ, Zamagni E, Morgan G, Dimopoulos MA, Durie BG, Anderson KC, Sonneveld P, San Miguel J, Cavo M, Rajkumar SV and Moreau P: Revised International Staging System for Multiple Myeloma: A report from International Myeloma Working Group. J Clin Oncol *33(26)*: 2863-2869, 2015. PMID: 26240224. DOI: 10.1200/JCO.2015.61.2267

30 Kim HD, Kim BJ, Kim HS and Kim JH: Comparison of the morphologic criteria (RECIST) and metabolic criteria (EORTC and PERCIST) in tumor response assessments: a pooled analysis. Korean J Intern Med, 2018. PMID: 29334722. DOI: 10.3904/kjim.2017.063

31 Varga C, Maglio M, Ghobrial IM and Richardson PG: Current use of monoclonal antibodies in the treatment of multiple myeloma. Br J Haematol *181(4)*: 447-459, 2018. PMID: 29696629. DOI: 10.1111/bjh.15121

32 Dyrberg E, Hendel HW, Al-Farra G, Balding L, Løgager VB, Madsen C and Thomsen HS: A prospective study comparing whole-body skeletal X-ray survey with ^{18}F-FDG-PET/CT, ^{18}F-NaF-PET/CT and whole-body MRI in the detection of bone lesions in multiple myeloma patients. Acta Radiol *6(10)*: 2058460117738809, 2017. PMID: 29123920. DOI: 10.1177/2058460117738809

33 Bolzoni M, Toscani D, Costa F, Vicario E, Aversa F and Giuliani N: The link between bone microenvironment and immune cells in multiple myeloma: Emerging role of CD38. Immunol Lett, 2018. PMID: 29702149. DOI: 10.1016/j.imlet.2018.04.007

34 Wang Y, Yee AJ, Sirard C, Landau S, Raje N and Mahmood U: Sodium fluoride PET imaging as a quantitative pharmacodynamic biomarker for bone homeostasis during anti-DKK1 therapy for multiple myeloma. Blood Cancer J *7(10)*: e615, 2017. PMID: 28984867. DOI: 10.1038/bcj.2017.95

35 Elliott BM, Peti S, Osman K, Scigliano E, Lee D, Isola L and Kostakoglu L: Combining FDG-PET/CT with laboratory data yields superior results for prediction of relapse in multiple myeloma. Eur J Haematol *86(4)*: 289-298, 2011. PMID: 21198866. DOI: 10.1111/j.1600-0609.2010.01575.x

36 Zamagni E, Nanni C, Mancuso K, Tacchetti P, Pezzi A, Pantani L, Zannetti B, Rambaldi I, Brioli A, Rocchi S, Terragna C, Martello M, Marzocchi G, Borsi E, Rizzello I, Fanti S and Cavo M: PET/CT improves the definition of complete response and allows to detect otherwise unidentifiable skeletal progression in multiple myeloma. Clin Cancer Res *21(19)*: 4384-4390, 2015. PMID: 26078390. DOI: 10.1158/1078-0432.CCR-15-0396

Received February 27, 2019
Revised March 21, 2019
Accepted March 25, 2019